Single-mode waveguides with SU-8 polymer core and cladding for MOEMS applications

Nordström, Maria; Zauner, Dan; Boisen, Anja; Hübner, Jörg

Published in:
Journal of Lightwave Technology

Link to article, DOI:
10.1109/JLT.2007.893902

Publication date:
2007

Document Version
Publisher's PDF, also known as Version of record

Single-Mode Waveguides With SU-8 Polymer Core and Cladding for MOEMS Applications

Maria Nordström, Dan A. Zauner, Anja Boisen, and Jörg Hübner, *Member, IEEE*

***Abstract*—Fabrication and optical characterization of single-mode polymeric embedded waveguides are performed. A specific material combination (SU-8 2005 as core and the modified SU-8 mr-L 6050XP as cladding) is chosen in order to obtain a small refractive index difference for single-mode propagation combined with the conventional fabrication method UV lithography to facilitate the integration of different types of optical detection methods on lab-on-a-chip systems. We analyze the behavior of the refractive index and carefully observe how the value of the refractive index can be tailored during processing. We show that we can fabricate waveguides with an index difference in the order of 10^{-3}, where both the core material and the cladding material are based on SU-8. The refractive index measurements are performed on thin polymeric films, while further optical characterizations are performed on waveguides with a height of 4.5 μm. We study the mode profiles of these waveguides and confirm that only the fundamental mode is excited. We also study the absorption spectra of the material in the wavelength range 800–1600 nm combined with cut-back measurements. We find that the waveguides have a propagation loss of 0.2–3 dB/cm in this wavelength range.**

***Index Terms*—Low stress, single-mode, SU-8, waveguides.**

I. Introduction

MANY lab-on-a-chip systems developed today rely on different types of optical detection or readout methods, where light is guided by waveguides. For example, the growth rate of cells can be detected by absorption of light transmitted through a microchannel [1]. Another example is the detection of fluorescence from prelabeled molecules [2]. Such systems would benefit from a monolithic fabrication where both the basis of the analysis system as well as the optical components are fabricated in the same material. So-called microoptoelectromechanical systems (MOEMS) devices require the integration of optical detection methods as well as optomechanical structures without the addition of extra process steps. Moreover, full integration of optical components with mechanical structures offers the advantage of removing the time-consuming alignment otherwise needed between the optomechanical structures and optical fibers. Currently, there is a high focus on the investigation of different polymeric materials for waveguides [3], [4]. Other groups have reported on the fabrication of multimode waveguides in SU-8 [5]–[7], and methods have been developed to decrease the optical losses of such waveguides [8]. Single-mode waveguides in SU-8 have also been fabricated before, using a variation of other polymers as cladding material [9]–[11]. The previous work done within the area clearly shows the high interest and suitability of SU-8 for integrated optical components [12]–[15]. However, materials with different intrinsic properties and structuring methods have been used as core and cladding, thereby not obtaining the aforementioned advantages of monolithic structures. Here, we report on the fabrication of single-mode embedded SU-8 waveguides in a homogenous platform with both the core and cladding fabricated from the same material basis.

The mr-L XP resist is a modified version of the SU-8 resist. It has specifically been developed by Micro Resist as a low-stress polymer, and we have confirmed that it can easily be structured into centimeter-sized areas and 3-D structures without cracking. As a material platform, mr-L XP is well suited for systems used for biochemical analysis, as it possesses very high chemical resistance and good mechanical stability. This is the material chosen for cladding as it can simultaneously be used for making microchannels and other required structures. For the waveguide core, we use standard SU-8. SU-8 is suitable as core layer since it possesses a low optical absorption of 0.5 dB/cm both at 1100 and 1300 nm, and the fabrication process is fast, simple, and cost-efficient.

Both SU-8 and mr-L XP are negative resists structured by UV lithography followed by a baking step to induce cross-linking. The fact that both the core and cladding material are based on the same chemistry and are structured with the same method is an advantage to the processing as it reduces most risks of failure, for example, due to problems with adhesion between the different layers. Furthermore, since both materials are processed under the same conditions, the risk of negatively affecting one material from the processing of the next is eliminated. Would monolithic fabrication not have been applied an alternative cladding material could have been polymethylmethacrylate (PMMA). However, PMMA can only be patterned into specific structures by etching or with nanoimprint lithography (NIL). However, SU-8 is not compatible with such etching protocols, and NIL is a technology where high-cost stamps are required, high temperatures that might degrade the optical properties of SU-8 are involved, and the sizes possible to fabricate are limited to a few micrometers [16]. This further shows the advantages of maintaining a homogenous material combination. Moreover, the small refractive index difference in the material combination we have chosen allows for the design

Manuscript received February 16, 2006; revised July 27, 2006.

The authors are with MIC—Department of Micro and Nanotechnology, Nano DTU, Technical University of Denmark, DK-2800 Kgs. Lyngby, Denmark (e-mail: man@mic.dtu.dk).

Color versions of one or more of the figures in this paper are available online at http://ieeexplore.ieee.org.

Digital Object Identifier 10.1109/JLT.2007.893902

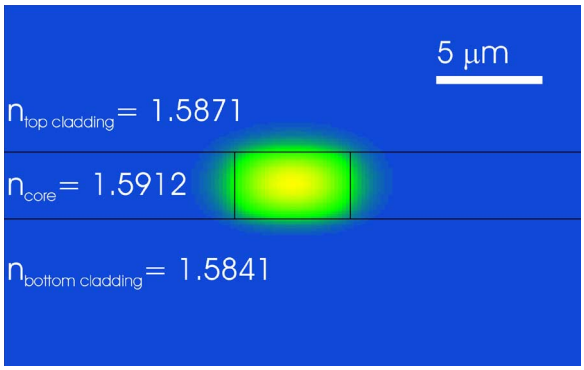

Fig. 1. Simulations from FiMMWAVE show the fundamental (TE00) mode at 635 nm for the 5-μm-wide and 4.5-μm-high waveguide. The slight asymmetry in the mode profile due to the refractive index difference between the top and bottom claddings can be noted.

of larger waveguides that still remain single mode. This is an advantage when butt-coupling the in-put fibers, as it is simply easier to see the waveguides during alignment. With respect to the optical properties, this material combination is highly suitable since the two polymers have a stress-optical coefficient of the same order, which ensures that the effective refractive index does not change significantly, even if the system is subject to stress, e.g., by heating.

II. Theoretical Simulations

The aim of this paper is to fabricate single-mode low-stress waveguides. We have performed theoretical simulations (FiMMWAVE, Photon Design, U.K.) of the mode profile of waveguides of widths up to 10 μm, as we want to combine the single-mode light propagation with a high throughput of light.

The simulations are performed at 635 nm, with respect to TE polarized light. All waveguides are embedded waveguides with a refractive index difference of 4×10^{-3} between the core and the top cladding and 7×10^{-3} between the core and the bottom cladding. Fig. 1 shows the simulation of the fundamental mode of a 5-μm-wide waveguide. From the BPM simulations, we see that the waveguide can support two guided modes in the horizontal plane, but the calculations show that the first-order mode is only weakly guided. It is therefore not very likely that more than the fundamental mode will be present when the waveguide is excited with a single-mode fiber. The height of all waveguides is 4.5 μm, and from our theoretical simulations, it can be seen that also two modes can be supported in the vertical direction at 635 nm.

The fabricated waveguides have square cores, which make the geometrical contribution to the birefringence negligible; hence, we have not investigated the birefringence of these polymer waveguides. We believe the contribution due to stress can be ignored for our application since the intrinsic stress of this material combination is low. For long macromolecular chains, the anisotropic orientation of the aromatic rings will lead to birefringence [17]. However, SU-8 is an isotropic material, cross-linking in a ladderlike structure, which makes this contribution negligible [18].

III. Experimental Details

A. Refractive Index Measurements

The refractive index of the polymers is measured using a prism coupler (Metricon 1020, Pennington, NJ, USA), which measures both the film thickness and refractive index using a fitting routine. We investigate how the refractive index can be tuned during the processing by varying the exposure dosage and cross-linking temperature. Films of both polymers are processed at 60 °C, 90 °C, or 110 °C. Simultaneously, different regions on the test wafers are exposed to different dosages of UV light: 180, 270, or 360 mJ/cm^2.

B. Film Stress Analysis

The stress of the polymer films is measured by using a profiler (Tencor P-1, Tenor Instruments, USA) and scanning the wafer before and after the polymers are deposited and cross-linked. This method utilizes the theory developed by Stoney [19], which relates the radius of curvature of the wafer to the stress of the thin film deposited. To induce further stress to the films, they are heated on hotplates to either 90 °C or 120 °C for 2 min.

C. Waveguide Fabrication

The SU-8 waveguides are fabricated using SU-8 2005 (MicroChem, Newton MA, USA) as the core material and the modified SU-8, mr-L 6050XP (Micro Resist Technology, Berlin, Germany) as both top and bottom cladding layer. The backbone of the chemical composition of mr-L XP and SU-8 is the same, but a plasticizer has been added to the mr-L XP to make the polymer more flexible and less susceptible to stress-induced cracks during the processing. Another difference between the two polymers is that they contain different solvents: cyclopentanone for SU-8 2005 and γ-butyrolacetone for mr-L 6050XP. Consequently, their processing parameters differ slightly, but the process sequence is the same. All structures are fabricated on top of 4-in Si wafers coated with a 3-μm-thick thermally grown oxide as optical buffer layer.

The first step of the process is spin-coating the mr-L 6050XP lower cladding layer to a thickness of 20 μm with a spin speed of 4000 r/min for 30 s. The layer is soft baked at 90 °C on a horizontally leveled hotplate. The polymer is exposed to 365-nm I line UV light and cross-links during the successive postexposure bake (PEB) for 20 min at 90 °C. The SU-8 2005 layer forming the waveguide core is spin-coated on top of the lower cladding layer to a thickness of 4.5 μm at a spin speed of 5000 r/min. The soft bake parameters are set to 10 min at 60 °C and, subsequently, 10 min at 90 °C. The waveguide structures are patterned by an exposure to 365-nm I line UV light. The following PEB uses the same settings as the soft bake. The nonexposed SU-8 is developed in propylene–glycol–methyl–ether–acetate (PGMEA), and the structures are rinsed with isopropanol. Finally, the top cladding, also consisting of mr-L 6050XP, is structured using the exact same process sequence as the lower cladding layer. Fig. 2 shows

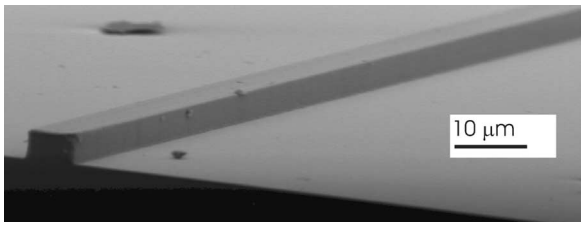

Fig. 2. SEM picture of a 4.5-μm-high and 5-μm-wide single-mode SU-8 waveguide.

a SEM image of a 4.5-μm-high and 5-μm-wide single-mode SU-8 waveguide.

During fabrication, the bottom cladding layer will have obtained a double exposure dosage compared to the top cladding layer. This results in a slight asymmetry in the refractive index profile of these waveguides.

D. Cut-Back Measurements

The losses of these waveguides are measured using the cut-back method for waveguides of varying widths: 3, 5, and 10 μm. All waveguides have a height of 4.5 μm. The length of the waveguide samples is cut back from 88 to 20 mm in four steps. The propagation loss is measured over the spectral range of 800–1600 nm, scanned at a resolution of 10 nm. The setup comprises a halogen lamp focused through a lens encapsulated in a metallic box to prevent the interference of the nonfocused light with the measurement. Light is butt-coupled into the waveguides with a 125-μm single-mode fiber (Corning, USA) with a core diameter of 9 μm and numerical aperture of 0.13. The output light is collected at the opposite end using the same coupling method, and the signal is analyzed using a spectrum analyzer (86140A, Hewlett Packard, USA). The white light used for the measurements is nonpolarized. Since the polarization dependent losses are generally not relevant for this type of application, we have not investigated this phenomenon.

From the results of the cut-back measurement over the spectral range of 800–1600 nm, specific absorption peaks can be identified, and the most suitable operational wavelength can be determined.

E. Mode Profiles

The mode profiles of the waveguides are measured using 635-nm light coupled into the waveguides with the same procedure as described above. The exiting light is projected onto a charge-coupled device camera (XCD-X710, Sony, Japan) using a 20× lens. The images are captured and analyzed with standard image analysis software (Image Tool, UTHSCSA). An example of the captured images is shown in the inset of Fig. 3.

IV. Results and Discussion

A. Refractive Index Measurements

We measure the variation in the polymer refractive index as a function of the processing temperature and exposure dosage. Fig. 4 clearly shows that the refractive index of the films is highly dependent on both the exposure dosage and the temperature at which it cross-links. This is an important feature of the device material, and care shall be taken to maintain all process conditions constant. By increasing the processing temperature from 60 °C to 110 °C, the refractive index is reduced by 2×10^{-3} on average for the differently exposed films of SU-8. Likewise, if the exposure dosage is increased by 180 mJ/cm^2, the refractive index is decreased by 1×10^{-3} on average for the different processing temperatures. However, the exposure dosage seems to have less effect when the films are processed at a lower temperature. The data for the mr-L XP films contain larger spreads, so no conclusive value can be obtained, but a clear trend is seen. However, it shall be remembered that the lower cladding layer will have obtained the double exposure dosage compared to the top cladding during fabrication. From further measurements with the prism coupler at 635 nm, mimicking the complete fabrication process, we find the refractive index to be 1.5912 for the waveguide core, 1.5871 for the top cladding, and 1.5841 for the lower cladding.

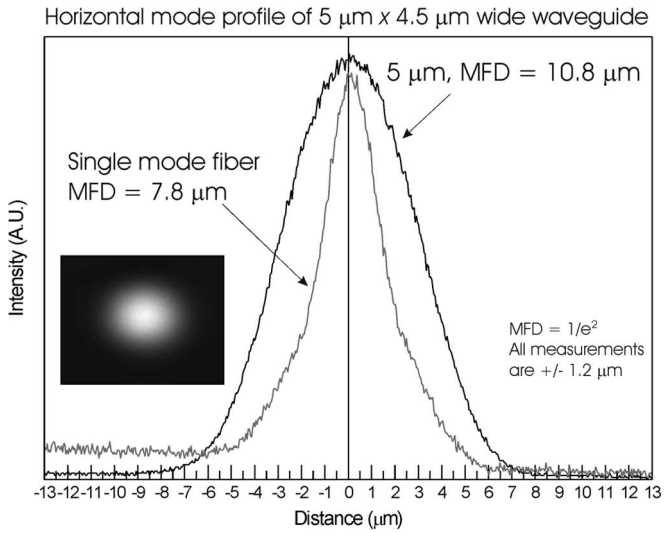

Fig. 3. Mode profile at 635 nm of a 5-μm-wide and 4.5-μm-high waveguide. For comparison, the mode profile of the 9-μm fiber is shown in gray at the center. The theoretically calculated mode field diameter of the 5-μm-wide waveguide is 9.6 μm, which compares well with the measured value. The inset shows the mode profile as it appears on the CCD camera. The light that is coupled into the waveguide is randomly polarized, but the birefringence of this waveguide is negligible.

B. Film Stress Analysis

It is known from photoelastic theory that stresses in a polymer film will affect the refractive index of the material [20], [21]. This, combined with the low-stress behavior of the mr-L XP film proposed by the suppliers, led us to investigate the stress of the two polymeric films when subject to external thermal stresses. Since the thicknesses of the films are very different, it is not relevant to compare the values of the stresses directly. Instead, the stress optical coefficient is calculated (see Fig. 5). From this graph, it is clearly seen that the value of the refractive index is inversely related to the stress for both polymers. SU-8 has a stress optical coefficient of 2.6×10^{-4} MPa^{-1}, and the value for the mr-L XP resist is

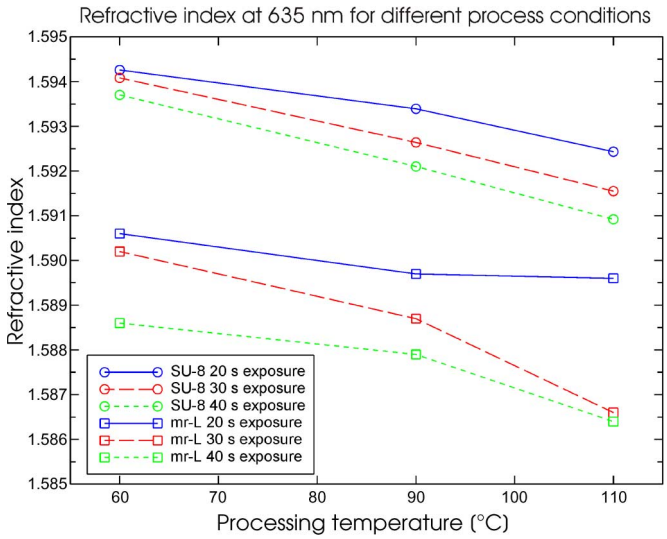

Fig. 4. The refractive index of the polymers that are used for core and cladding is highly dependent on the processing temperature and the exposure dosage, as shown. However, the refractive index of the two materials follows the same trend with reduced values as a result of both higher exposure dosage and cross-linking temperature.

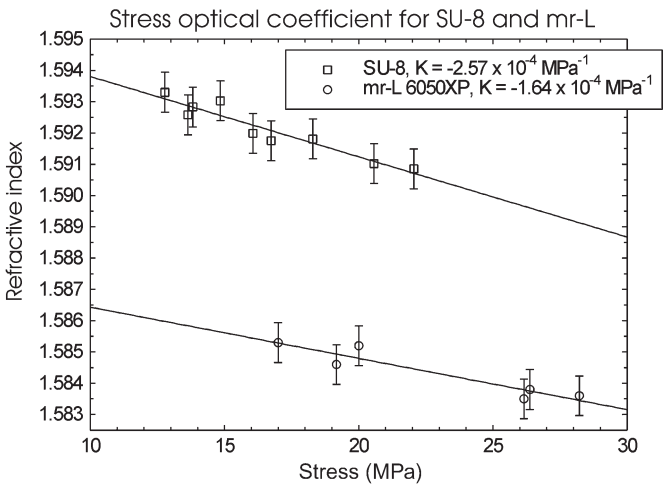

Fig. 5. Stress optical coefficient for the core material (SU-8) and the cladding material (mr-L 6050XP). The stress optical coefficient is calculated as $\kappa = \Delta n/\Delta\sigma$, where n is the refractive index and σ is the stress in the polymer film. The value is slightly lower for the cladding material. The stress in the film is calculated from Stoney's equation [16], i.e., $\sigma_f = (E_s/(6(1-\upsilon_s)))(t_s^2/t_f)(1/R)$, where E_s is the Young's modulus of the substrate, υ_s is the Poisson ration of the substrate, t_s and t_f are the thicknesses of the substrate and the polymer film, respectively, and R is the radius of curvature of the wafer.

slightly lower: 1.6×10^{-4} MPa^{-1}. The values are of the same magnitude, which ensures that the refractive index difference of the waveguides will remain constant, even if the system is subject to heat cycles.

The induced stresses in the films are seen to be relaxed and stable after three days. However, the value of the refractive index is lower than the initial value, typically around 0.05%. This indicates that the refractive index variations are not only caused by thermal stress changes. One suggestion we investigated is the absorption of water into the polymer matrix. It was initially believed that water is evaporated during the bake steps and then reabsorbed, leading to the observed increase in the refractive index. This proposition was rejected though, as the same trend in the refractive index variation is observed when the test wafers are stored in a N_2 container. The reduction in the refractive index could be due to residuals of solvents in the polymers that are evaporated during the heating steps, thereby reducing the refractive index. However, these slight variations should not decrease the reliability of systems fabricated in these materials as such drastic temperature changes are not usually applied during standard biochemical analyses.

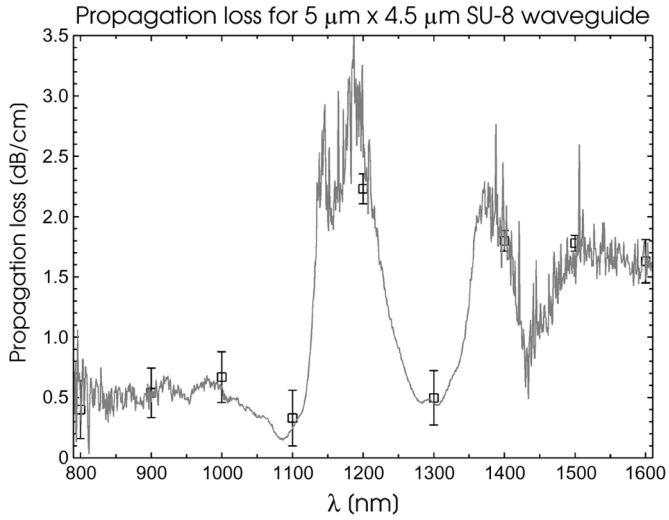

Fig. 6. The propagation loss for a 5-μm-wide and 4.5-μm-high single-mode waveguide in SU-8 is plotted in the spectral range of 800–1600 nm. As shown, the waveguide is best operated around 1090 or 1300 nm. Error bars are marked for every 100 nm. The white light that is used for the measurements is not polarized, but the birefringence of this waveguide is negligible.

C. Cut-Back Measurements

Fig. 6 shows the results obtained from the cut-back measurements over the spectral range 800–1600 nm. For clarity, only the data obtained from the 5-μm-wide waveguide is plotted. The propagation loss varies between 0.2–3 dB/cm over the spectra.

As can be seen from the graph, the propagation loss of these SU-8 waveguides is in general low, but due to the excitation of molecular vibrations in the chemical structure of the waveguide material, there are certain regions that have a significantly higher absorption. SU-8 is an organic material with high absorption in the far infrared region. However, each bond will also have several overtones in the near-infrared part of the spectra, as seen below. At 1140 nm, there is an absorption peak for the C–H bond in the aromatic ring of the SU-8. The CH_3 group shows absorption at 1190 and 1360 nm. In the region 1470–1600 nm, the absorption is also very high. This region corresponds to overtones of the R–OH bonds generated from the epoxy groups formed during the cross-linking of the SU-8. Additionally, the peak is due to the combination overtones of the second-order stretching and deformation of the aromatic rings. From the cut-back measurements, it can be seen that the lowest absorption of the SU-8 is around 1090 and 1300 nm.

The coupling loss between the fiber and the waveguide has a value of ~5 dB/facet for the 3-μm-wide waveguide,

$\sim$3 dB/facet for the 5-μm-wide waveguide, and only $\sim$1 dB/facet for the 10-μm-wide waveguide. We have not investigated the polarization-dependent losses.

D. Mode Profile Analysis

Fig. 3 shows the horizontal mode profiles of a 5-μm-wide waveguide and, for comparison, a 9-μm fiber. The theoretical simulations show an expected mode field diameter of 9.6 μm for the 5-μm-wide waveguide, and the measured value of 10.8 μm is well within the error margin. From the mode profiles, we can conclude that using butt coupling and proper alignment, only the fundamental mode is excited even for the waveguide with the maximum width of 10 μm.

V. Conclusion

Here, we present a first stage optical characterization of single-mode waveguides fabricated monolithically in the polymeric material SU-8, which is suitable for MOEMS applications. We have also studied how the refractive index is affected by changes in the processing and further heat treatments. We show that waveguides of this type can easily be fabricated by UV lithography, which allows for the fast fabrication of complex lab-on-a-chip systems with integrated optics. Furthermore, we show that these waveguides have a low propagation loss of 0.2 dB/cm at 1090 nm and 0.5 dB/cm at 1300 nm and that only the fundamental mode of the waveguides is excited.

Acknowledgment

The authors would like thank M. Svalgaard at the Department of Communications, Optics, and Materials, Technical University of Denmark (DTU), for the loan of the white light source for the spectral analysis.

References

[1] R. A. Yotter, L. A. Lee, and D. M. Wilson, "Sensor technologies for monitoring metabolic activity in single cells—Part II: Nonoptical methods and applications," *IEEE Sens. J.*, vol. 4, no. 4, pp. 395–411, Aug. 2004.

[2] R. Marie, S. Schmidt, A. Johansson, L. Ejsing, M. Nordström, D. Häfliger, C. B. Christensen, A. Boisen, and M. Dufva, "Immobilisation of DNA to polymerised SU-8 photoresist," *Biosens. Bioelectron.*, vol. 21, no. 7, pp. 1327–1332, Jan. 2006.

[3] B.-H. V. Borges and L. E. M. de Barros, Jr., "Design of optical biosensor using polymeric waveguides," in *Proc. IEEE Int. Microw. Optoelectronics Conf.*, 1999, vol. 1, pp. 66–69.

[4] X. Lu, C.-H. Jang, D. An, Q. Zhou, L. Sun, X. Zhang, R. T. Chen, and D. Dawson, "Polymeric multimode waveguide based electro-optic modulator with a vertically configured dumping planar waveguide," *Appl. Phys. Lett.*, vol. 81, no. 5, pp. 795–797, Jul. 2002.

[5] K. B. Mogensen, J. El-Ali, A. Wolff, and J. P. Kütter, "Integration of polymer waveguides for optical detection in microfabricated chemical analysis systems," *Appl. Opt.*, vol. 42, no. 19, pp. 4072–4079, Jul. 2003.

[6] J. M. Ruano, M. Aguirregabiria, M. Tijero, M. Arroyo, J. Garcia, J. Berganzo, I. Arambur, F. J. Blanco, and K. Mayora, "Monolithic integration of microfluidic channels and optical waveguides using a photodefinable epoxy," in *Proc. MEMS*, 2004, pp. 121–124.

[7] M. Nathan, O. Levy, I. Goldfarb, and A. Ruzin, "Monolithic coupling of a SU-8 waveguide to a Silicon photodiode," *J. Appl. Phys.*, vol. 94, no. 2, pp. 7932–7934, 2003.

[8] B. Bêche, P. Papet, D. Debarnot, E. Gavio, J. Zyss, and F. Poncin-Epaillard, "Fluorine plasma treatment on SU-8 polymer for integrated optics," *Opt. Commun.*, vol. 246, no. 1–3, pp. 25–28, Feb. 2005.

[9] B. Bêche, N. Pelletier, E. Gaviot, and J. Zyss, "Single-mode $TE_{00} - TM_{00}$ optical waveguides on SU-8 polymer," *Opt. Commun.*, vol. 230, no. 1–3, pp. 91–94, Jan. 2004.

[10] K. K. Tung, W. H. Wong, and E. Y. B. Pun, "Polymeric optical waveguides using direct ultraviolet photolithography process," *Appl. Phys. A, Solid Surf.*, vol. 80, no. 3, pp. 621–626, Feb. 2005.

[11] B. Y. Shew, C. H. Kuo, Y. C. Huang, and Y. H. Tsai, "UV-LIGA interferometer biosensor based on the SU-8 optical waveguide," *Sens. Actuators A, Phys.*, vol. 120, no. 2, pp. 383–389, May 2005.

[12] D. A. Chang-Yen and B. K. Gale, "An integrated optical oxygen sensor fabricated using rapid-prototyping techniques," *Lab Chip*, vol. 3, no. 4, pp. 297–301, Nov. 2003.

[13] J. Hsieh, C.-J. Weng, H.-L. Yin, H.-H. Lin, and H.-Y. Chou, "Realization and characterization of SU-8 micro cylindrical lenses for in-plane micro optical systems," *Microsyst. Technol.*, vol. 11, no. 6, pp. 429–437, Jun. 2005.

[14] C.-J. Lin and F.-G. Tseng, "Micro Fabry-Pérot sensor for nano-lateral displacement sensing with enhanced sensitivity and pressure resistance," *Sens. Actuators A, Phys.*, vol. 114, no. 2/3, pp. 163–170, Sep. 2004.

[15] F. J. Blanco, M. Agirregabiria, J. Berganzo, K. Mayora, J. Elizalde, A. Calle, C. Domínguez, and L. M. Lechuga, "Microfluidic-optical integrated CMOS compatible devices for label-free biochemical sensing," *J. Micromech. Microeng.*, vol. 16, no. 5, pp. 1006–1016, May 2006.

[16] D. Nilsson, T. Nielsen, and A. Kristensen, "Solid state microcavity dye lasers fabricated by nanoimprint lithography," *Rev. Sci. Instrum.*, vol. 75, no. 11, pp. 4481–4486, 2004.

[17] J. Jiang, C. L. Callender, C. Blachetière, S. Jacob, J. P. Noad, J. Ding, Y. Qi, and M. Day, "Optimizing fluorinated poly(arylene ether)s for optical waveguide applications," *Opt. Mater.*, vol. 28, no. 3, pp. 189–194, Feb. 2006.

[18] J. M. Shaw, D. D. Gelorme, N. C. LaBianca, W. E. Conlye, and S. J. Holmes, "Negative photoresists for optical lithography," *IBM J. Res. Develop.*, vol. 41, no. 1/2, pp. 81–94, 1997.

[19] G. G. Stoney, "The tension of metallic films deposited by electrolysis," *Proc. R. Soc. Lond.*, vol. 82, no. 553, pp. 172–175, 1909.

[20] S.-K. Kim, K. Geary, W. Yuan, H. R. Fetterman, D.-G. Lee, C. Zhang, C. Wang, W. H. Steier, G.-C. Park, S.-J. Gang, and I. Oh, "Stress-induced polymer waveguides operating at both 1.31 and 1.55 μm wavelengths," *Electron. Lett.*, vol. 40, no. 14, pp. 866–868, Jul. 2004.

[21] S. Agan, F. Ay, A. Kocabas, and A. Aydinli, "Stress effects in prism coupling measurements of thin polymer films," *Appl. Phys. A, Solid Surf.*, vol. 80, no. 2, pp. 341–345, Feb. 2005.

Maria Nordström received the B.Sc. (Hons.) degree in physics from Imperial College of Science, Technology, and Medicine, London, U.K., in 2001, and the M.Sc. degree in physics from Lund University, Lund, Sweden, in 2003. She is currently working toward the Ph.D. degree at the Technical University of Denmark, Lyngby, Denmark, focusing on the field of polymeric lab-on-a-chip systems with emphasis on cantilever-based sensors.

Dan A. Zauner received the M.Sc. degree in physics from the University of Copenhagen, Copenhagen, Denmark, in 1996, and the Ph.D. degree in optical telecommunication from the Department of Communications, Optics, and Materials, Technical University of Denmark, Lyngby, Denmark, in 1999.

Before being employed at the Department of Micro and Nanotechnology in 2004, where he worked toward the integration of surface-enhanced Raman spectroscopy with on-chip spectroscopy, he worked for Corning, Corning, NY, and NKT A/S, DK.

Anja Boisen received the M.Sc. degree in physics from the University of Roskilde, Roskilde, Denmark, in 1993, and the Industrial Ph.D. degree in micromechanics from the Department of Micro and Nanotechnology (MIC), Technical University of Denmark, Lyngby, Denmark, and the company Danish Micro Engineering A/S, Denmark, in 1997.

Since 1997, she has been an Assistant Research Professor with MIC, and since January 1999, she has been Associate Professor and Project Leader of the Bioprobe project. In January 2005, she was appointed Full Professor and Leader of the Nano Systems Engineering section with MIC. She has a thorough knowledge on micromechanics and nanotechnology and has more than 10 years experience in microfabrication and cantilever-based sensing.

Jörg Hübner (M'99) received the M.Sc. degree in electrical engineering from University of Stuttgart, Stuttgart, Germany, in 1994, and the Ph.D. degree in photonics from the Department of Micro and Nanotechnology (MIC), Technical University of Denmark (DTU), Lyngby, Denmark, in 1998.

After two years of postdoctoral work within integrated optics, he became Group Leader and Associate Professor of the integrated lightwave circuits group at the Department of Communications, Optics, and Materials, DTU. In 2001, he moved to Silicon Valley to work as Senior Engineering Manager with Sparkolor Corporation. Returning to DTU, in 2002, he joined MIC in 2003 to work on integrated Raman spectroscopy sensor systems. In 2005, he was appointed Deputy Director of MIC.